Assessment of wind conditions at a fjord inlet by complementary use of sonic anemometers and lidars

Jakobsen, Jasna Bogunovic ; Cheynet, Etienne ; Snæbjörnsson, Jonas ; Mikkelsen, Torben; Sjöholm, Mikael; Angelou, Nikolas; Hansen, Per; Mann, Jakob; Svardal, Benny ; Kumer, Valerie

Total number of authors:
11

Published in:
Energy Procedia

Link to article, DOI:
10.1016/j.egypro.2015.11.445

Publication date:
2015

Document Version
Publisher's PDF, also known as Version of record

Available online at www.sciencedirect.com

ScienceDirect

Energy Procedia 80 (2015) 411 – 421

Energy Procedia

12th Deep Sea Offshore Wind R&D Conference, EERA DeepWind'2015

Assessment of wind conditions at a fjord inlet by complementary use of sonic anemometers and lidars

Jasna Bogunović Jakobsen[a,*], Etienne Cheynet[a], Jonas Snæbjörnsson[a,b], Torben Mikkelsen[c], Mikael Sjöholm[c], Nikolas Angelou[c], Per Hansen[c], Jakob Mann[c], Benny Svardal[d], Valerie Kumer[e], Joachim Reuder[e]

[a]*Department of Mechanical and Structural Engineering and Materials Science, University of Stavanger, N-4036 Stavanger, Norway*
[b]*School of Science and Engineering, Reykjavik University, Menntavegur 1, 101 Reykjavk, Iceland*
[c]*Department of Wind Energy, Technical University of Denmark, Ris Campus Frederiksborgvej 399, DK-4000 Roskilde, Denmark*
[d]*dChristian Michelsen Research AS, Fantoftveien 38, Bergen, Norway*
[e]*Geophysical Institute, University of Bergen, Allegaten 70, N-5007 Bergen, Norway*

Abstract

Wind velocity measurement devices based on the remote optical sensing, lidars, are extensively applied in wind energy research and wind farm operation. The present paper demonstrates the relevance and potential of lidar measurements for other wind-sensitive structures such as long-span bridges. In a pilot study in Lysefjord, Norway, a pulsed long-range lidar and two short-range WindScanners were installed at the bridge site, together with a long-term monitoring system based on sonic anemometers. The deployment of the two types of lidars is described in more details and the complementary value of the data from all three types of the instruments is illustrated. The emphasis is on the lidars' potential to map the wind conditions along the whole span of a bridge in a complex terrain, as opposed to "point" measurements achievable by sonic anemometers. The challenging balance between the spatial and temporal resolution of the data is discussed.

Peer-review under responsibility of SINTEF Energi AS

Keywords: Long-range pulsed lidar, Short-range WindScanner, Sonic anemometer, Length-scale, Coherence, Long-span bridges

1. Background

Wind measurement devices based on optical remote sensing have been extensively developed over the past thirty years, in the last years largely in response to the demands of the wind energy industry for resource mapping at increasing heights and offshore. Applications of lidars in wind energy include both fundamental studies of the wind turbine inflow and investigations of the downstream wake field characteristics, and use static and scanning ground-based as well as nacelle mounted lidars. The latter have also been exploited for wind forecasting, power curve assessment and adaption of the feed-forward control strategies. An overview over the international advancement in

* Corresponding author. Tel:+47-51831666 ; fax: +47-51831750.
E-mail address: jasna.b.jakobsen@uis.no

Peer-review under responsibility of SINTEF Energi AS
doi:10.1016/j.egypro.2015.11.445

the lidar-based wind measurements, with emphasis on the research activities at the Danish Technical University Risø Campus, is presented in [1].

The main focus of the lidar-based wind field studies has been on the slowly varying flow characteristics such as wind profile and turbulence intensity. More limited efforts have been dedicated to the investigation of the flow characteristics at shorter time scales, e.g. in terms of fine-turbulence (cross-) spectra. This is due to the inherent spatial averaging by lidars and a trade-off between the spatial and the temporal resolution when deploying the scanning lidars. A low-pass filtering effect of the spatial averaging on the single point spectral tensor has been investigated both analytically and experimentally in [2] and [3]. In [4], deployment of a long-range pulsed lidar in offshore conditions and its performance regarding the turbulence measurements is reported. Other studies have dealt with lidar based coherence estimates, analyzing fixed single-beam data ([5], [6], [7]) or synthetized "two-dimensional" records ([7]), using the Taylor hypothesis of "frozen" turbulence. While certain characteristics of turbulence can be deduced from the measurements with a single lidar, several synchronized instruments can naturally better resolve the temporal and spatial flow characteristics. This approach is fundamental when studying the details of the complex flow structures such as the rotorcraft downwash [8].

Similarly to its significance in wind energy, turbulence is among the governing load factors in the design of long-span bridges and other slender, wind sensitive structures. Both temporal and spatial characteristics of turbulence are fundamental for the total load and the dynamic response. The wind field characterization by lidars is therefore very relevant to long-span bridges, and the present work describes a pilot project demonstrating the potential of corresponding lidar-based measurements. The paper describes the experiences and results of a measurement campaign at the Lysefjord bridge in South-West Norway, performed in spring 2014. The long-term measurement system on the bridge, based on the ultrasonic anemometers, was complemented by a long-range pulsed lidar and two synchronized continuous-wave short-range WindScanners. A secondary goal of this novel activity was to stimulate the development of new lidar-based measurement setups and corresponding data interpretation strategies. The paper focuses on the description of the measurement campaign and the presentation of selected preliminary results.

1.1. The measurement site and the long-term wind monitoring system

Fig. 1 shows the Lysefjord suspension bridge, with the main span of 446 m, immersed in complex terrain at the fjord inlet. A smaller, embedded picture displays the 40 km long fjord, which is 2 km wide at the most and 600 m narrow at the bridge location. The bridge stretches from the North-West (NW) to the South-East (SE). The hills on both sides of the fjord have slopes of 30-45 °, reaching 350 m in height to the North and 600 m to the South. The fjord alignment and its connection to the outer Høgsfjord to the SW define two main wind directions at the bridge site, i.e. the S-SW and the NE wind directions.

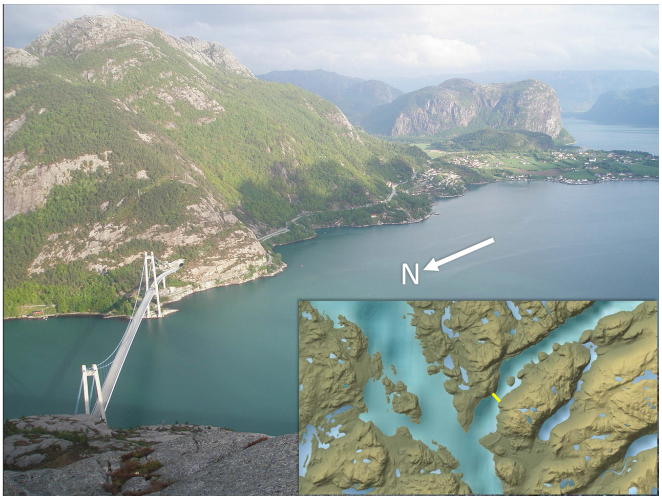

Fig. 1. Map of Lysefjord area (bridge shown by a yellow line) and a photo of the fjord inlet taken from Stokkanuten in North [9].

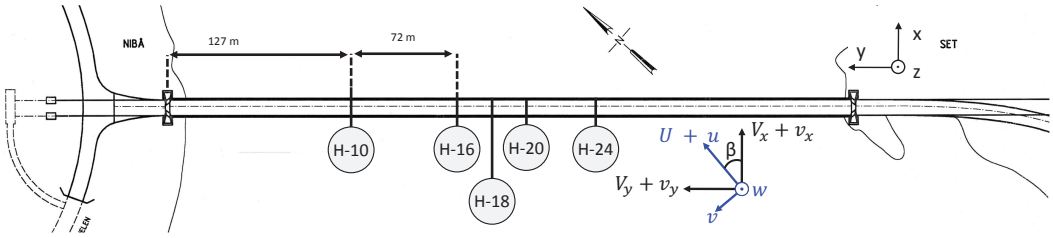

Fig. 2. Wind velocity components and the location of the five sonic anemometers. H-18 is located exactly in the middle of the bridge span.

The long-term monitoring system includes both ultrasonic anemometers and accelerometers and was installed in 2013 as part of a research project on wind-induced vibrations of long-span bridges. The project is managed by the University of Stavanger (UiS) and supported by the Norwegian Public Road Administration (NPRA). The wind monitoring system consists of five sonic anemometers distributed over a distance of 168 m, as depicted in Fig. 2. One of them is a 2D Vaisala Weather Sensor WXT520 and the remaining four sensors are 3D sonic anemometers by Gill (Wind MatsterPro 1561-PK-020). Two of the instruments are fixed to the vertical hangers, which connect the bridge deck to the main cables. In the central part of the span, where the hangers are too short to provide the support for instruments that can capture the unobstructed flow, the anemometers were supported directly on the top of the main suspension cables. The anemometers were deployed from the walkway at the South-West side of the bridge, approximately 6 m above the bridge deck, i.e. at an elevation of 60.5 m above sea level. The WindMaster-Pro anemometers record the wind velocity data at a rate of 32 Hz, and the Vaisala Weather station at hanger H-10 samples data at the rate of 4 Hz.

In Fig. 2, the horizontal mean wind velocity component at an arbitrary angle to the normal to the bridge β is designated U, and the turbulence components (u, v and w) presented following the associated wind-based coordinate system. The vertical mean wind velocity is here assumed zero for simplicity, although this is generally not the case. In addition to the "wind-based" coordinate system, the wind velocity components referring to the bridge coordinate system (V_x+v_x, V_y+v_y and w) are also presented. This is because the turbulence component normal to the bridge span, v_x, and its simultaneous appearance along the bridge span, i.e. the co-coherence, governs the total instantaneous force exerted on the bridge. The bridge deck itself is built as a "streamlined" closed steel-box and aerodynamically behaves similarly to a "flat-plate". In addition to the horizontal turbulence normal to the bridge, vertical turbulence is thus significant for generation of the lift force and the overturning moment. The lowest eigen-frequencies of the bridge are 0.13 Hz, 0.30 Hz and 1.24 Hz for the first symmetric lateral, vertical and torsional modes respectively. Beside the resonant response, the quasi-static response to the slowly varying turbulence is also important, the so-called background response.

2. Wind flow characterization by a long-range pulsed Doppler lidar

In 2014, University of Stavanger, University of Bergen, Christian Mikkelsen Research and Leosphere, all partners in NORCOWE (Norwegian Research Centre for Offshore Wind Energy) developed a joint research activity, exploring the performance of a long-range pulsed lidar in bridge engineering. As opposed to the fine-structure turbulence sensing by sonic anemometers clustered over a relatively short portion of the bridge span, in order to provide a good data source for the co-coherence estimates, the long-range lidar can be used to survey the whole bridge span. It can therefore give a good indication of the possible effects of the fjord topography on the homogeneity of the flow. In the planning phase, prior to the construction of a bridge, long-range lidars can be used to link the flow conditions at the very bridge site, where it crosses the fjord, to in-situ measurements by anemometers typically installed on a mast at a fjord side.

From March to June 2014, a long-range pulsed Doppler lidar with a steerable laser beam (WindCube 100S) was operating from the roof of the Lysefjord center, 1.75 km SW from the bridge, at an elevation of 5.7 m. Four scanning modes were applied: (a) Doppler Beam Swinging mode (DBS) for wind profile monitoring, (b) Plan Position Indicator mode (PPI) for scans over an azimuth sector at a fixed elevation, (c) Range Height Indicator mode (RHI) for

measurements at a fixed azimuth and varying elevation, and (d) the Sequential Fixed Line of Sight mode (LOS) for measurements along a single line. The first three modes were typically combined in a sequence lasting for one hour and investigating the homogeneity of the flow. The PPI mode was applied at three elevations (0.8°, 1.8° and 3.2°), covering the heights of 30.2 m, 60.7 m and 103.6 m at the bridge location. The azimuth sector from 13° to 63° (see Fig. 3) was monitored in steps of 1° per 0.2 second, giving a resolution of 31 m along the bridge. The radial resolution in this mode was 25 m and a maximum scanning distance 2440 m from the lidar. The RHI scans were run at three azimuth angles, targeting the center of the bridge and the areas in the proximity of the pylons. The elevations were varied from 0° to 6° in steps of 0.6°, giving a vertical resolution of 18 m at the bridge site. In May, during a one week period, the LOS measurements with a radial resolution of 25 m were carried out, pointing at the central part of the bridge span.

In the following, selected measurement results from May 22, 2014 are presented. For reference, the mean horizontal wind velocity and the associated along-wind turbulence intensities are given in Fig. 4, in which the thick black line indicates the bridge alignment. The two prevailing wind directions, imposed by the fjord topography (from S-SW and NE) are evident. As expected, the turbulence intensity decreases with an increase in wind speed, but also depends on the wind direction, varying throughout the day.

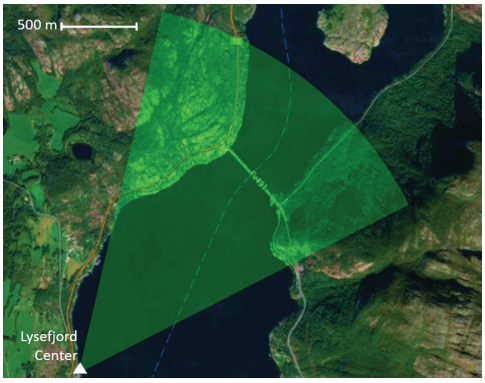

Fig. 3. Azimuth sector from 13° to 63° covered by the PPI scans by the long-range pulsed lidar.

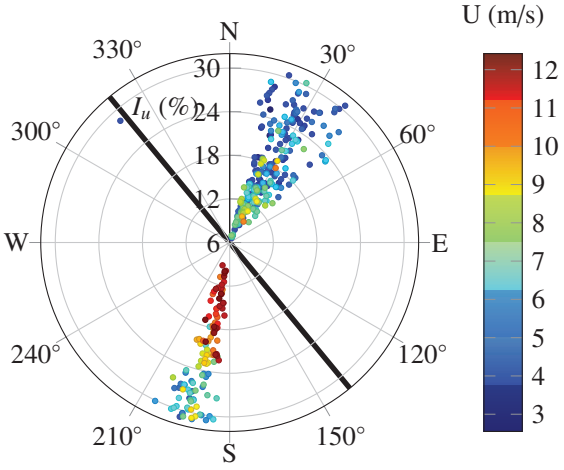

Fig. 4. Mean wind speed and turbulence intensity recorded by the sonic anemometers on 22.5.2014.

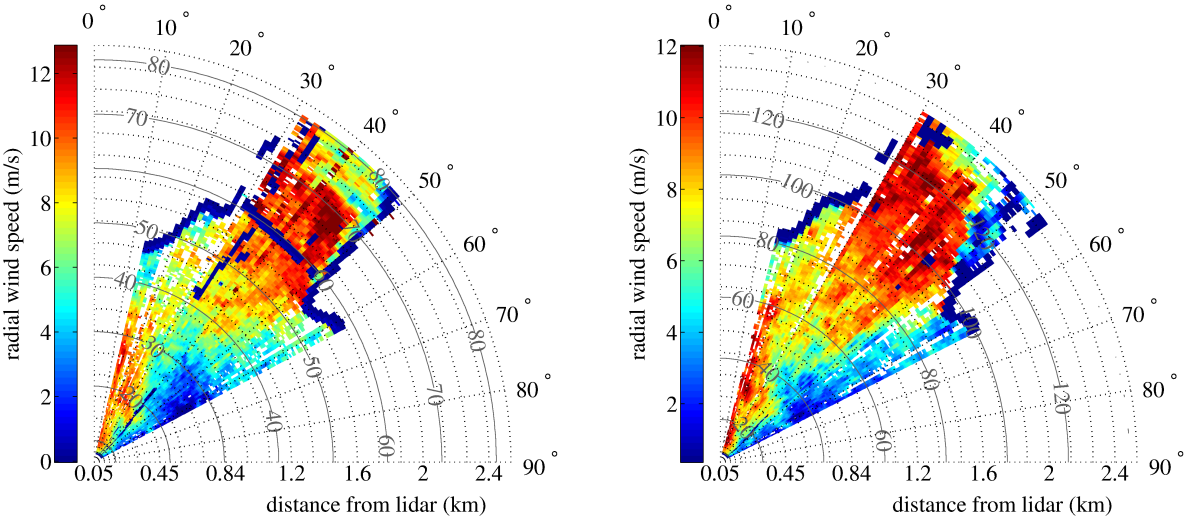

Fig. 5. Plan Position Indicator (PPI) mode data recorded on 22.5.2014, at 17:19:10 at the elevation of 1.8° (left) and at 17:19:23 at the elevation 3.2° (right). The radial grey contour plot indicates the altitude above the sea level (in meters).

In Fig. 5, the PPI data are presented for two elevations. The radial velocity measured by the lidar at the elevation of 3.2° (right panel) is on average higher compared to the data for elevation of 1.8° (left panel). At 1.8°, the measurement disturbances by the bridge are notable, including a distortion effect of the two towers. One should recall that the monitored elevations increase linearly with the distance from the lidar. Despite of this and the fact that the data only capture the radial velocity component, the scans indicate flow acceleration through the fjord "contraction" and a partial flow "veering" imposed by the steep terrain at the North-West side of the fjord. The mean wind direction at the time was about 190°, i.e. from South.

In Fig. 6, the spatial variation in the radial velocity upstream of the bridge is studied in terms of the correlation coefficient of the velocities at varying "lateral" separations, parallel to the bridge, recorded over a period of 10 minutes. The radial velocity data analyzed are for the volumes corresponding to the locations of the five sonic anemometers on the bridge, i.e. for the cells separated by tangential distances of 0 m, 60 m, 90 m, 120 m and 180 m, measured from the 37° degrees azimuth angle "pointing" towards the bridge hanger nr. 10. Because of the distorting effect of the bridge on the measurements, the velocities investigated are for the volumes 30 m upstream of the bridge. The corresponding correlation coefficient, from the sonic anemometers data, is also presented in Fig. 6, together with the exponential curves fitted to the correlation coefficients in the least square manner.

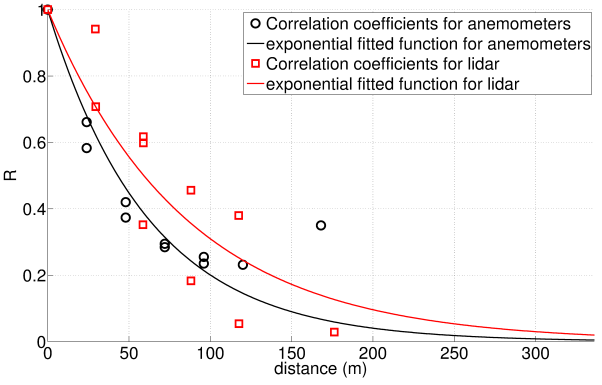

Fig. 6. Cross-correlation coefficient for the velocity component normal to the bridge as a function lateral separation, 17:15 to 17:25, 22.05.2014.

The general trend of the correlation coefficient from the lidar data is in agreement with the results from the sonic anemometers. The integral of the correlation coefficient, i.e. the area under the curves, corresponds to a length scale of approximately 60 m. However, the scatter in the coefficients based on the long-range pulsed lidar data is too high and does not reduce when analyzing the data from a larger number of monitored volumes. This is not surprising, since the PPI lidar data studied were sampled at time intervals as long as 80 s and thus captured only a basic variability in the turbulence time-series. Such a long time-interval was required for a scanning pattern chosen to include the PPI scans at three different elevations and three RHI scans. Estimates of the correlation coefficient are expected to improve if measuring the radial wind velocity in a dedicated PPI scanning sequence, with a shorter scanning pattern repetition time.

An example of the LOS data, sampled at 1Hz along a line pointing towards the middle of the bridge span at an azimuth angle of 39° is presented as a function of time, in Fig. 7. Various time-scales of gustiness can be observed. The same data but restricted to a position 30 m upstream of the bridge are presented in Fig. 8, together with the simultaneous time-series of the velocity component v_x observed by three of the sonic anemometers. In the figure, the lidar data have been shifted by approximately 3 s, in order to account for the estimated average travel time over the 30 m distance to the measurement "points" along the bridge. The agreement between the data obtained by the two different measurement methods and very different distances from the sensing point or volume is satisfying and promising for further studies. Table 1 gives the data comparison in terms of the mean radial wind velocity and its standard deviation.

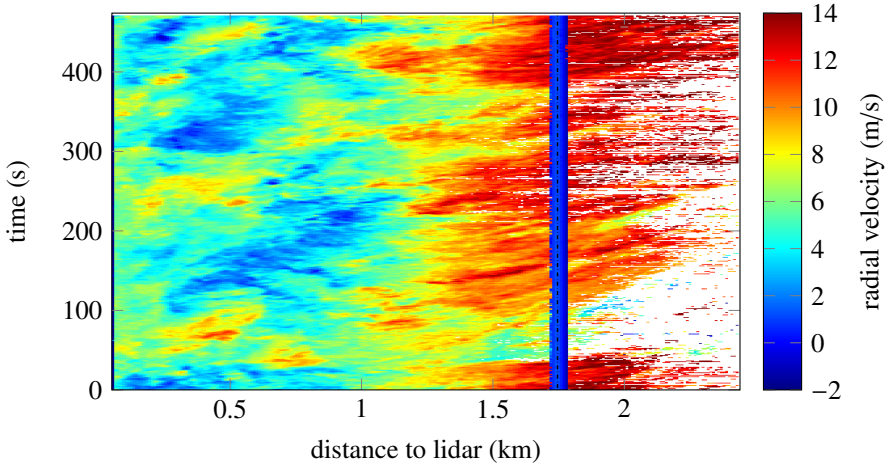

Fig. 7. Sequential Fixed Line of Sight mode (LOS) measurement, elev=1.8 azim=39, radial velocity recorded from 16:12:06, 22.05.2014.

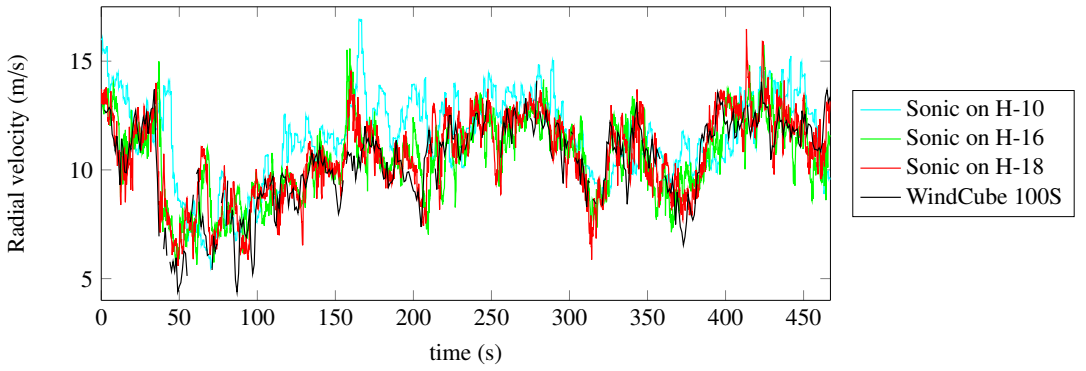

Fig. 8. Radial wind velocity recorded by a LOS scan and by the sonic anemometers 30 m further downstream from 16:12:06, 22.05.2014.

Table 1. Basic statistics of the wind velocity data presented in Fig. 8

Sensors	Mean radial speed (m/s)	RMS radial speed (m/s)
Long-range pulsed lidar	10.4	1.8
Anemometer at H-10	11.5	2.1
Anemometer at H-16	10.5	1.8
Anemometer at H-18	10.6	1.9

3. Flow characterization by the short-range WindScanners

In May 2014, two synchronized short-range WindScanners developed by the Technical University of Denmark, based on a modified ZephIR 150 lidar, were deployed on the bridge walkway on the West side, for a period of one week. The activity was developed as research collaboration between Christian Michelsen Research, the University of Stavanger, the Danish Technical University, and the University of Bergen. Fig. 9 shows the WindScanner positioned in the Northern part of the bridge span, pointing towards South.

The two WindScanners were placed at a distance of 90 m between them, centered around the middle of the bridge span. The two instruments monitored the wind field primarily in the horizontal plane, mapping the inflow conditions for the wind coming from S-SW and the wake of the bridge girder, in case of the wind from NE. They were synchronized so that the intersection point of the two lines of sight moved forth and back along a 120 m long line 40 m upstream of the bridge, at a scanning pattern repetition rate of about 1 Hz. The 120 m long measurement domain implied a continuous change in the focusing distance for the two WindScanners and the size of the volume over which the velocity is averaged. This was accounted for when extracting the horizontal velocity field from the WindScanner data, similarly to the data analysis described in [6]. In a limited number of the tests, the lidars were monitoring the flow in a nearly vertical plane, in an attempt to further characterize the bridge girder wake. The LOS mode with a fixed line of sight was also employed. The Doppler spectra were averaged such that LOS wind velocities were provided at about 390 Hz.

Fig. 10 depicts the velocity components normal to (v_x) and parallel to (v_y) the bridge axis, over a period of 2.5 minutes. The increase in the velocity component normal to the bridge and the associated velocity decrease parallel to the bridge (and vice versa) visualize fluctuations in the wind direction. The large gusts appear to be rather coherent over the 120 m measurement domain. A positive distance along the bridge denotes the Southern part of the bridge span. A systematic delay in gust arrivals at the North end of the monitored line is consistent with the mean wind direction of 190, estimated from the 10 minutes ultrasonic anemometer data.

Fig. 9. Short-range WindScanner deployed from the bridge walkaway.

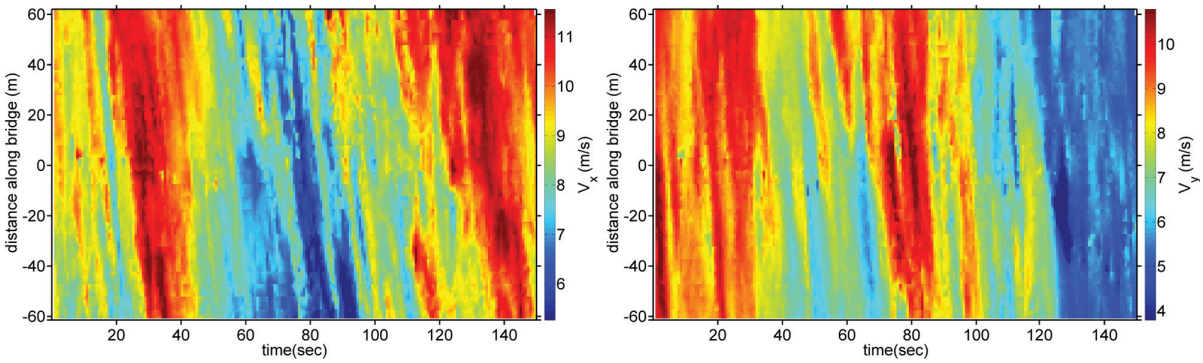

Fig. 10. Wind velocity normal (left) and parallel to the bridge (right) as observed by the WindScanners, starting at 16:20, 22.5.2014

A direct comparison between the WindScanner velocity data and the sonic anemometer data is presented in Fig. 11, demonstrating a high consistency between the two data sets. The 40 m long distance between the measurement domains for the two types of instruments is accounted for by adjusting the time axis of the WindScanner data by about 4 s.

Fig. 12 gives a comparison of the power spectral densities of the horizontal wind fluctuations along the mean wind direction u and normal to it v, computed from the WindScanners and the anemometer data. The spectral values $F_i(k_1)$, i= u, v, are presented as functions of the wave number $k_1=2\pi f/U$ in a product format, $k_1F_i(k_1)$. The 120 m long domain monitored by Wind Scanners was discretized into cells of 5 m length, and the spectral estimate presented is based on the data from all of the observation cells, acquired over a 20 minutes long period. The analysis is performed by dividing the 20 minutes time series into blocks of 10 minutes data and averaging the results for the two periods. The spectral estimates presented for the sonic anemometer data are calculated by averaging the spectra from five anemometers, for the data recorded simultaneously with the analyzed WindScanners time-series. A very good agreement between the pairs of the spectra can be observed. For wave numbers higher than approximately 0.02, the spectra based on the lidar records underestimate the spectral values calculated from the sonic anemometer data, a discrepancy which increases with an increasing wave number. This is an expected effect of the spatial averaging of the velocities within the scanning volume.

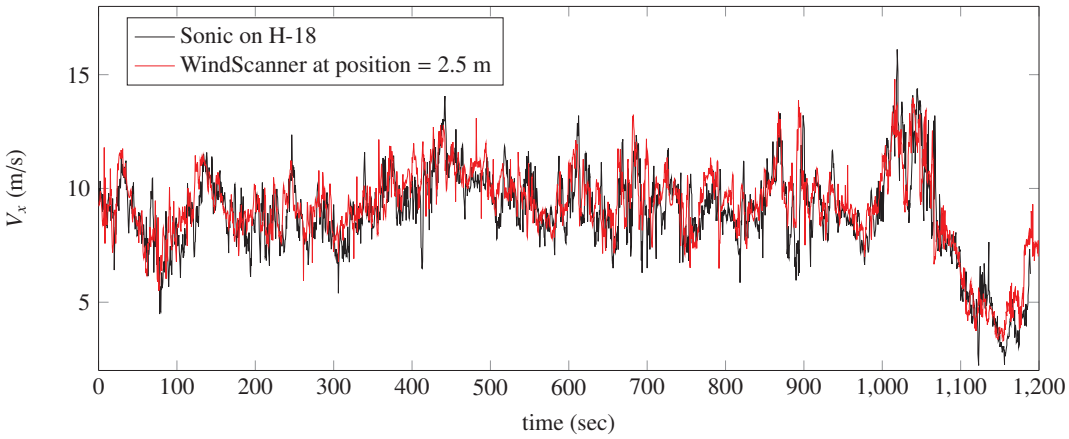

Fig. 11. Wind velocity normal to the bridge as observed by the WindScanners and the sonic anemometer, starting at 16:20, 22.5.2014.

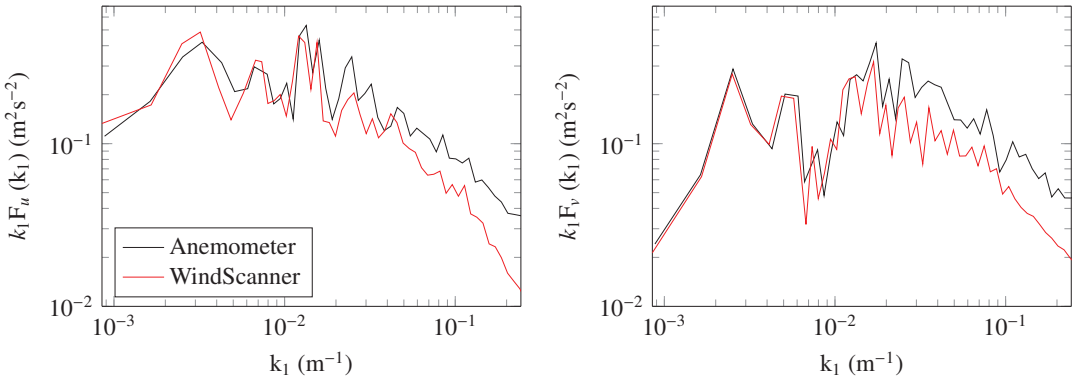

Fig. 12. Power spectral density of the longitudinal (left) and lateral turbulence (right), based on 20 minutes data starting at 16:20, 22.5.2014.

Based on the agreement between the WindScanners data and the sonic anemometer data demonstrated in Fig. 11 and Fig. 12, the associated coherence functions are also expected to be consistent. The squared coherences for pairs of the WindScanners velocity records are presented in Fig. 13, as functions of the product between the wave number and the distance between the points projected in the across-flow direction, D. The time-series analyzed are for the period studied in Fig. 11 and 12, extended to a total duration of 30 minutes. For the along-wind component, the coherences for different separations D decay in a unified manner, as commonly found in the case of relatively large length scales. For the lateral turbulence, the coherence functions of k_1D are more spread for different distances D.

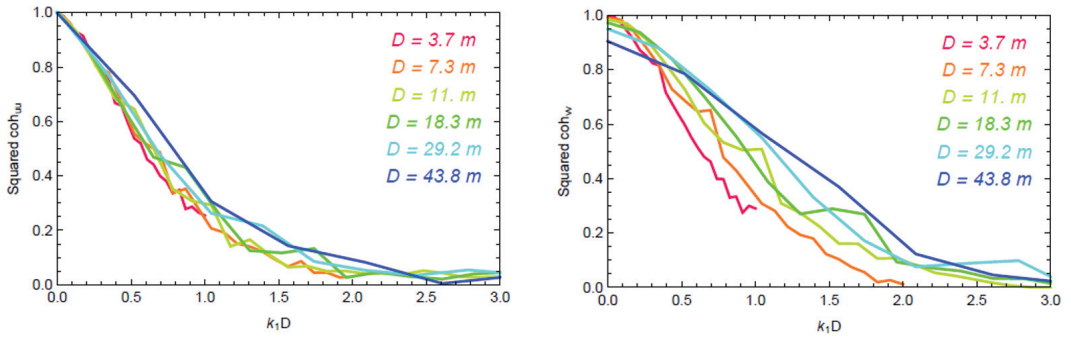

Fig. 13. Squared coherence based on the WindScanners data for the along-wind turbulence (left) and the lateral turbulence (right).

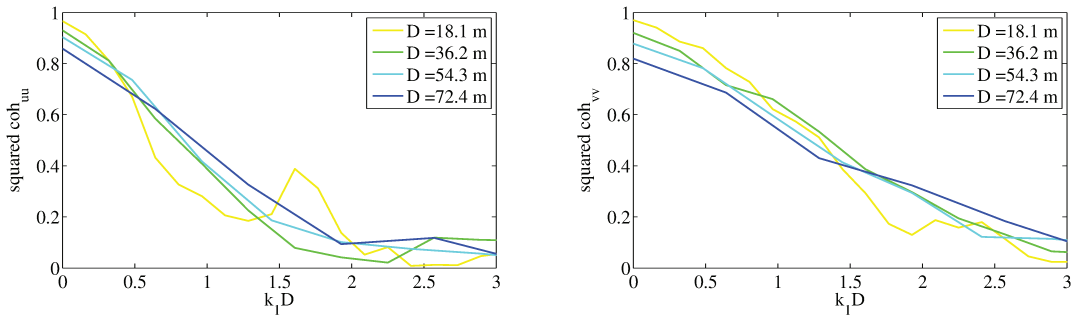

Fig. 14. Squared coherence based on the sonic anemometer data for the along-wind turbulence (left) and the lateral turbulence (right).

In Fig. 14, the corresponding results are given for the wind velocity data acquired by the sonic anemometers, for the time interval discussed in Fig. 11 and 12. The overall agreement between the normalized cross-power spectral densities based on the WindScanners data and the sonic data is good. One of the distinctions is that the sonic data capture a decreasing coherence at very low frequencies, in contrast to the lidar data which, for the longitudinal turbulence component, suggest the full coordination at the lowest frequencies investigated. This may be due to the smoothing effect of the lidars when measuring over a volume rather than a point, or due to the fact that the large number of time-series pairs analysed does not represent an ensemble of independent realizations. The auto-spectrum of the longitudinal turbulence measured by the sonic anemometers suggests a length scale in the order of 150-200 m, i.e. rather large compared to other studies (e.g. [10]).

The results presented demonstrate a significant potential of measurements with two synchronized short-range WindScanners to capture coherent flow structures as well as the spatial structure of turbulence in terms of the squared coherence function. The fast flow sensing outside the bridge structure itself, compared to the traditional use of sonic anemometers fixed to a bridge, offers new possibilities for studying the true flow approaching the bridge and the way that the flow interacts with the structure. Other examples of the acquired data and the in-depth comparison of the co-spectral estimates by WindScanners and the sonic anemometers will be presented in forthcoming publications.

The turbulence coherent structures measured upwind from a bridge deck bears also relevance for assessment of the turbulence wind conditions affecting wind loads on wind turbines operating offshore. Detailed coherent structure measurements as achieved here from two time and space coordinated short-range WindScanners could also be achieved offshore from fixed platforms such as transformers oil rigs. In addition, the long-range (pulsed) lidar can also measure wind conditions from fixed offshore platforms in or near offshore wind farm.

The presented results demonstrate that the turbulence spectra derived from the short-range WindScanners data are correctly represented at low-frequencies. The low-frequency velocity fluctuations constitute the major part of the turbulence variance, and are important for wind turbine wake meandering and several rigid body modes of a floating wind turbine. Higher frequency turbulence components, relevant to bottom fixed wind turbines and the flexible modes of a floater, are attenuated in the presented spectra. This stems from the spatial averaging of turbulence, when measuring at distances ranging from 40 m to 112 m, from the WindScanners. The smaller focusing distances in this range are thus preferable, where possible. Correction of the recorded data, using the theoretically and experimentally established lidar filtering characteristics, may also be used to improve the interpretation of the recorded velocity fluctuations.

4. Conclusions

The present paper describes a measurement campaign at the Lysefjord bridge, located in the South-West of Norway, carried out in spring 2014. The work was spurred off by the rapid development of the wind measurement techniques based on optical remote sensing, and the aim was to demonstrate their relevance for the upcoming fjord crossings project in Norway. It represents a novel cross-disciplinary activity, by introducing measurement techniques established in wind energy and other engineering fields into bridge engineering. Thereby, new lidar-based measurement setups and the corresponding data interpretation were explored.

The long-range lidars enable an investigation of the slowly varying wind conditions along the whole span of the structure, and are thus useful to study the possible impact of complex terrain on the uniformity of the flow across a fjord. The LOS data investigated are consistent with the corresponding local data acquired by sonic anemometers, and provide some insight into the wind gustiness. The PPI data, which were acquired with a scanning sequence repetition time of 80 s, provided limited information on the correlation of wind velocity in volumes separated in the lateral direction, which is of interest for bridge design. The result is expected to improve by wind measurements in a dedicated PPI scanning sequence, with a shorter scanning pattern repetition time. The use of a pair of synchronized long-range lidars is desirable to give an additional dimension to such data in the future.

In contrast to a low temporal resolution of the long-range lidars, overseeing large distances, the short-range WindScanners based on continuous-wave lidars can track much faster changes in the wind velocity over a selected area, and are suitable for studies of finer scale turbulence. The short-range WindScanners in the present study capture well the coherent structures in the flow, and give plausible co-spectral estimates of the horizontal velocity components. The in-depth comparison of the co-spectral estimates by the WindScanners and the sonic anemometers will be subject of

future work. The fast scanning short-range lidars deployed on the bridge encourage further studies of flow-structure interaction, by surveying the flow conditions in areas inaccessible by sensors fixed to the bridge structure. The experiences of such a campaign are also useful for future offshore campaigns, as the described methods can be applied to study offshore wind loads in greater detail.

Acknowledgements

The measurement campaign presented in the paper was supported by the Norwegian Public Road Administration, which also provided an important assistance during the deployment of the wind measurement systems at the bridge site. The realization of the measurements would not have been possible without the research network and support by NORCOWE, funded by The Research Council of Norway (project number: 193821). The in-kind contribution by Leosphere, facilitating the deployment of a long-range pulsed lidar, is greatly acknowledged.

References

[1] Mikkelsen, T.. Lidar-based research and innovation at dtu wind energy? a review. In: Journal of Physics: Conference Series; vol. 524. IOP Publishing; 2014, p. 012007.
[2] Mann, J., Cariou, J.P., Courtney, M.S., Parmentier, R., Mikkelsen, T., Wagner, R., et al. Comparison of 3d turbulence measurements using three staring wind lidars and a sonic anemometer. In: IOP Conference Series: Earth and Environmental Science; vol. 1. IOP Publishing; 2008,.
[3] Sathe, A., Mann, J.. Turbulence measurements using six lidar beams. In: 16th International Symposium for the Advancement of Boundary-Layer Remote Sensing. 2012, p. 302–305.
[4] Canadillas, B., Bégué, A., Neumann, T.. Comparison of turbulence spectra derived from lidar and sonic measurements at the offshore platform fino1. In: Proceedings of the 10th German Wind Energy Conference, DEWEK. 2010,.
[5] Kristensen, L., Kirkegaard, P., Mann, J., Mikkelsen, T., Nielsen, M., Sjöholm, M.. Spectral coherence along a lidar-anemometer beam. Tech. Rep.; Danmarks Tekniske Universitet, Risø Nationallaboratoriet for Bæredygtig Energi; 2010.
[6] Sjöholm, M., Kapp, S., Kristensen, L., Mikkelsen, T.. Experimental evaluation of a model for the influence of coherent wind lidars on their remote measurements of atmospheric boundary-layer turbulence. In: SPIE Remote Sensing. International Society for Optics and Photonics; 2011,.
[7] Lothon, M., Lenschow, D.H., Mayor, S.D.. Coherence and scale of vertical velocity in the convective boundary layer from a doppler lidar. Boundary-layer meteorology 2006;121(3):521–536.
[8] Sjöholm, M., Angelou, N., Hansen, P., Hansen, K.H., Mikkelsen, T., Haga, S., et al. Two-dimensional rotorcraft downwash flow field measurements by lidar-based wind scanners with agile beam steering. Journal of Atmospheric and Oceanic Technology 2014;31(4):930–937.
[9] https://upload.wikimedia.org/wikipedia/commons/4/45/Lysefjordbroen_sett_fra_Sokkanuten.jpg; 2010. Accessed: 2015-01-30.
[10] EN 1991-1-4: Eurocode 1: Actions on Structures, General Actions: Wind Loads. 1991.